DOE/CS/34153-2

# COOL POOL DEVELOPMENT

Grant No. DE-FG02-77CS34153

formerly Grant Number DE-FG04-79CS34153

Quarterly Technical Report #2

June through Dec. 1979

January 5, 1980



KAREN CROWTHER, AUTHOR

LIVING SYSTEMS
ROUTE 1, BOX 170
WINTERS, CA 95694

## DISCLAIMER

# C O O L  P O O L  D E V E L O P M E N T

Grant Number DE-FG04-79CS34153

Quarterly Technical Report #2

June through Dec. 1979

January 5, 1980

KAREN CROWTHER, AUTHOR

LIVING SYSTEMS
ROUTE 1, BOX 170
WINTERS, CA 95694

## INTRODUCTION

Air conditioners are the cause of peak electrical demand for many parts of the United States. (1) In dry areas evaporative cooling can relieve this demand. Conventional evaporative coolers ("swamp coolers") absorb the air's heat to evaporate water, thus lowering the air temperature. This increases the humidity which can reduce the occupants' feelings of comfort.

Indirect evaporative cooling eliminates the humidity problem by using an intermediary heat exchanger between the water source and the conditioned air. Interior air can be circulated through heat exchanger pipes located within an evaporative cooler as shown in figure 1.

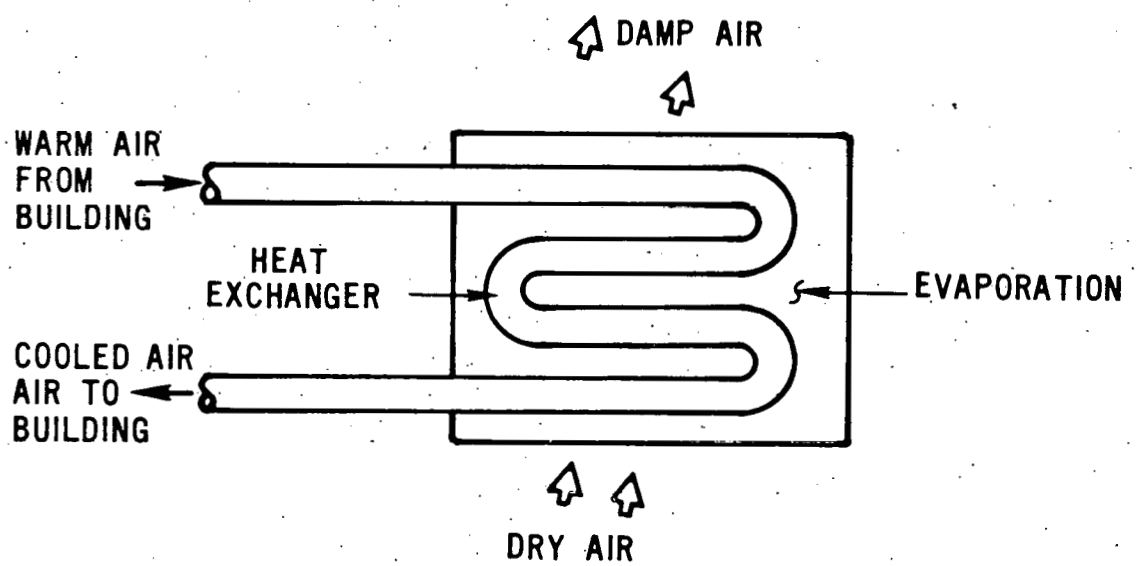


Figure 1. Indirect Evaporative Cooler

Or, an evaporating roof pond can be used to cool a building ceiling which absorbs heat from the living space by convection and radiation. (See figure 2)

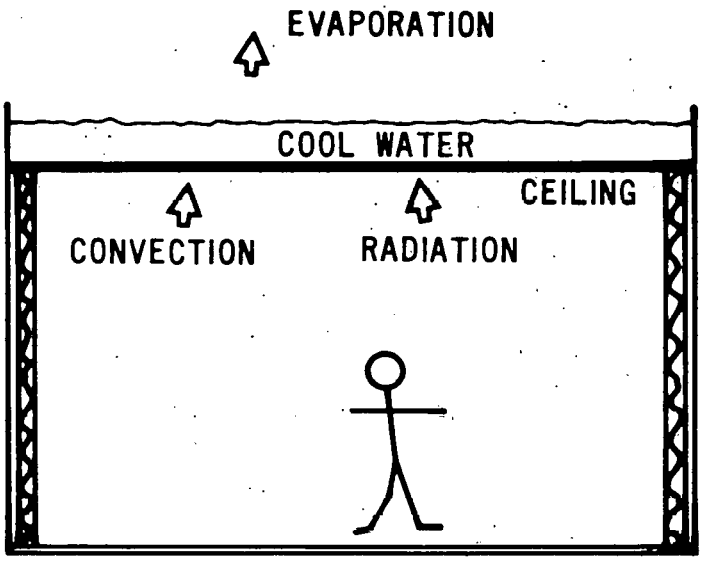


Figure 2. Roof Pond

The Cool Pool is a variation of the evaporating roof pond idea. The pool is isolated from the living space and the cooled pond water thermosiphons into the water columns located within the building. (See figure 3)

This report will discuss a computer model of the "Cool Pool" and the various heat and mass transfer mechanisms involved in the system. Theory will be compared to experimental data collected from a Cool Pool test building.

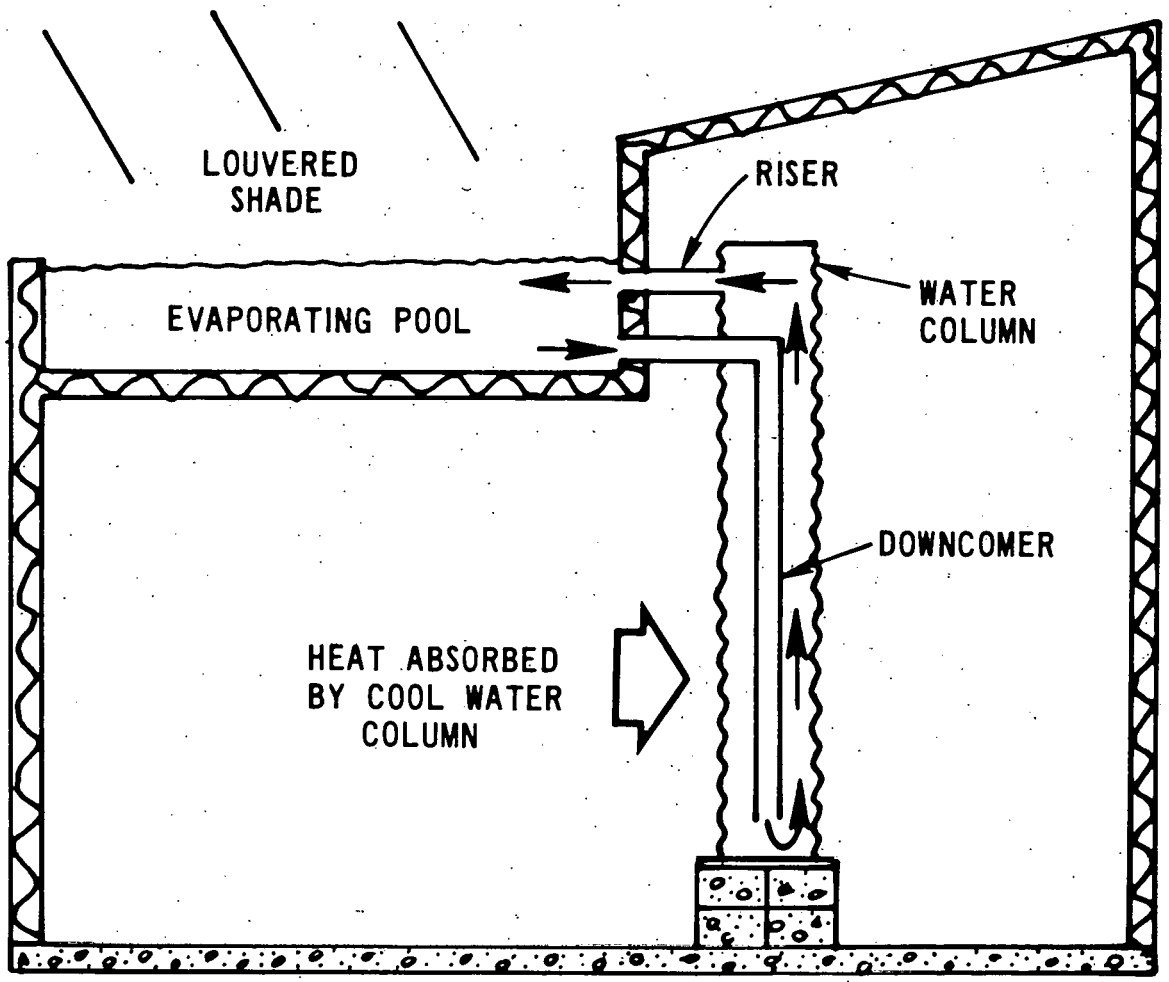


Figure 3. Cool Pool

## HOW IT WORKS

Figure 3 shows a schematic of the Cool Pool which consists of a shaded, evaporating roof pond connected to a column of water located within the building. The top connecting pipe (the riser) delivers warm water from the column to the pool. The lower connecting pipe (the downcomer) runs from the pool bottom, to the bottom of water column. The downcomer is placed within the water column to reduce the visible plumbing and improve the appearance of the system.

Evaporation keeps the roof pond cool. In the Central Valley of California where the weather is dry and hot the pool will usually remain between 60-70°F (15-21°C).

The water column which is absorbing heat from the building interior will be warmer than the pool. This sets up a density difference between the water column and the pool and downcomer. This density difference between two columns of water creates a pressure difference which causes the cool, dense water from the pool to flow through the downcomer into the bottom of the water column. The warmed water in the column rises and flows out the riser into the pool.

The greater the pressure difference the faster the water circulates. This pressure difference is a function of temperature (the warmer the water column is compared to the pool and downcomer the faster the flow). The pressure difference is also dependent on height so that the longer the downcomer is (provided it still contains cooler water) the faster the flow will be.

The water column remains cooler than the inside air due to the circulation of water from the roof pond. It acts to cool the living space by convection to the air and radiation to the interior objects and walls. In this model, conduction to the floor was negligible

although it might be desirable to design the column to maximize conduction.

The presence of the cold water column within the living space not only cools the environment but provides a heat sink to which people can radiate. Since radiation is a significant heat rejection mechanism for people this aids in their feelings of thermal comfort. (3)

## EXPERIMENTAL SET-UP

A Cool Pool building was monitored to verify the accuracy of the heat transfer relationships and the computer program.

The Cool Pool is installed on a 12' x 12' (3.66 m x 3.66 m) building with R-19 walls, R-30 roof and R-5 insulation around the perimeter of the concrete slab floor. (See Appendix 1 for the plans). The ceiling is 91" (2.31 m) high under the roof pond and slopes up to 147" (3.73m) at the highest point. The 24 sq. ft. ($2.2m^2$) of south windows are insulated with R-5 wood shutters. A 60 square foot ($3.57\ m^2$) roof pond is located on the north side of the roof under black louvered 3/8" plywood shades which block direct sun but allow free air movement over the pool. The roof pond is a galvanized steel pan, insulated on the sides and bottom.

The water columns are fabricated from 16 gauge corrugated galvanized steel culverts with metal plates welded to the bottom. The top end is sealed with opaque polyethylene taped to prevent air leakage. Four columns, 8' (2.44 m) tall and 1 1/2' (.457m) diameter are placed on plywood over cinderblocks in the building. The two columns farthest east were emptied and not used in these experiments.

Each column is connected to the roof pool by 1 1/2" (3.8 cm) I.D. galvanized pipes. After the downcomer enters the column a 90° ABS elbow connects it to the 65" (1.65 m) tall 1 1/2" diameter, 1/4 inch thick, ABS descending pipe.

Temperatures were measured with 30 gauge Omega Copper-Constantan thermocouple wires which were welded together and coated with epoxy to guarantee accurate readings under water. Since temperature changes were slow, sensor response time was not an important factor. The

thermocouples were constructed from a single spool of wire and calibrated with an HP digital voltmeter in a Rosemount controlled ice bath and hot oil bath. The thermocouples showed uniform readings (±.001 mV at most). They agreed with the platinum resistance thermometer to well within 0.05°C at 10°C and 20°C. They were uniformly biased at 30°C by +0.1°C and at 40°C by +0.2°C.

Net radiation into the roof pond was monitored with a one year old Weather Measure R422 Net Radiometer. The factory calibration constant was used. Outside wet bulb temperature was monitored with an aspirated, platinum resistance wet bulb thermometer and double-checked with a recording hygrothermograph.

Sensor readings were processed and recorded with a Fluke 2200B data logger.

Figure 4 shows the thermocouple placement. Temperatures were measured at 5 heights within the water column, 3 heights within the downcomer, 8 heights in the interior air. A thermocouple was taped to each wall, two places on the roof, and on the floor.

The thermosiphoning rate was measured by injecting dye into a rubber sleeve which connected a 4 foot (1.22 m) long 1 1/2" (3.8 cm) I.D. clear tube to the riser outlet. The Boussunesq relation gives:

$$\text{length for fully developed flow} = .03\ Re \cdot D$$

where: Re = Reynolds number

D = pipe diameter

For the velocities measured this length was between 2 and 3 feet. Therefore the injected dye was timed between the 3 ft. and 4 ft. marks on the clear tube. Flow was always laminar so the centerline velocity was timed and divided by 2 to yield the average velocity.

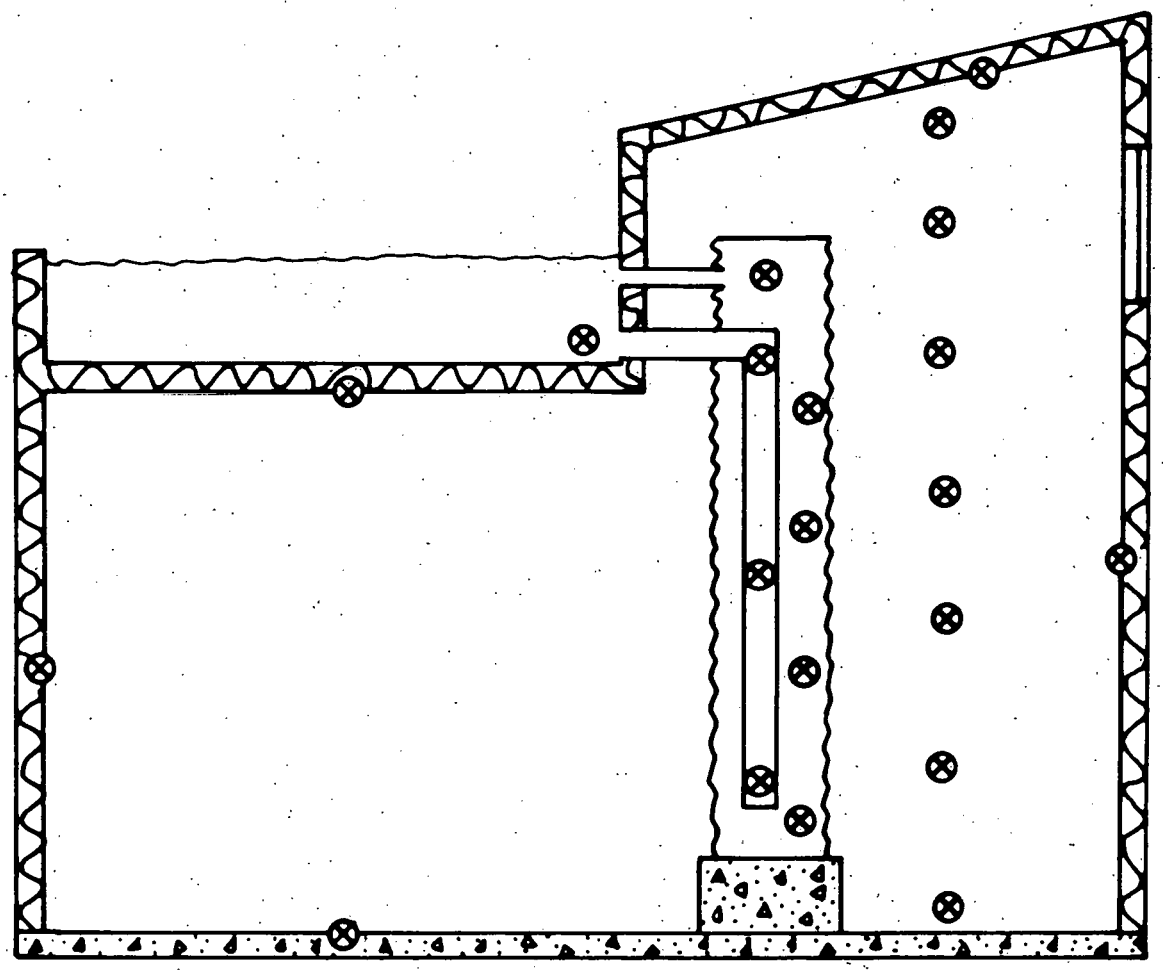

Figure 4. Thermocouple Placement

Measurements were not taken until the system was set up for at least three days.

## HEAT AND MASS TRANSFER PATHS

Before the Cool Pool computer model was developed the various heat and mass transfer processes were studied individually. Figure 5 shows the main heat and mass transfer paths for the Cool Pool system.

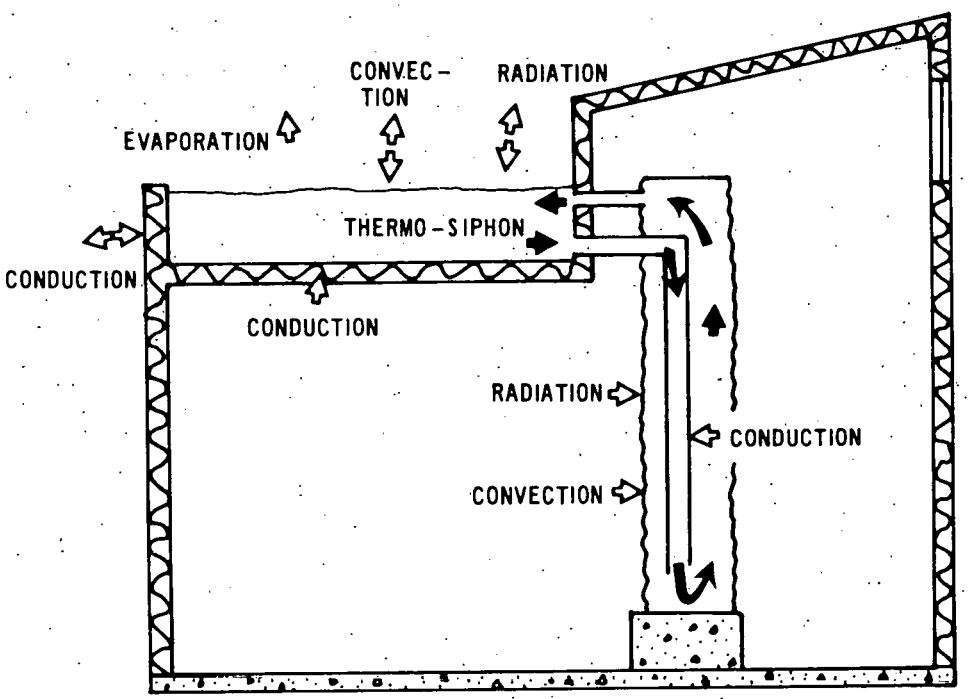


Figure 5. Heat and Mass Transfer

Heat is transfered into the water column by convection from the air and radiation from the walls, people, furniture, windows, etc. In this system the windows were shuttered and no insolation fell on the columns.

Mass is transported from the pool, through the downcomer and column and out into the pool via the riser. Heat is conducted and convected into the downcomer from the column water.

The pool water is primarily cooled by evaporation. Depending on outside conditions, it is either cooled or heated by convection, radiation and conduction.

## THERMOSIPHONING

Thermosiphoning hot water systems have been studied by Baughn, Dougherty and Crowther (2,3,4) as well as others.

The pressure difference caused by the density variation between two columns of water can be related to the flow velocity by the following equation:

$$\text{(eq. 2)} \quad \int \gamma dh_{cold} - \int \gamma dh_{warm} = \gamma \frac{v^2}{2g} \left( f \frac{L}{d} + K \right)$$

where

$\int \gamma dh_{cold}$ = the water density times differential height integrated over the height of the column of cooler water

$\int \gamma dh_{warm}$ = the density-height product integrated over the height of the column of warm water

$\gamma$ = water density

h = height

v = velocity

g = gravity

f = friction factor for pipe losses

L/d = length to diameter ratio for pipe

K = expansion factor used in figuring pipe frictional losses

The right side of this equation is the conventional expression for the pressure drop due to flow within a pipe.

For laminar flow the friction factor, f, can be found from the following relationship

$$\text{(eq. 3)} \quad f = 64/Re$$

where Re is the Reynolds' number based on the pipe diameter.

Flow through the 1 1/2" (3.8 cm) diameter column was found to create very little friction compared to the flow through the downcomer and riser. The L/d ratio was 120 and the expansion factor, K, was 4.0. A second order curve fit relates the viscosity and density of water to its temperature.

(eq.4) $\gamma(\#/ft^3) = 62.3302 + 6.706x10^{-3}T(°F) - 1.016x10^{-4}T^2 \quad [60°F < T < 79°F]$

(eq. 5) $\nu(ft^2/sec) = 2.7897x10^{-5} - 3.491x10^{-7}T(°F) + 1.458x10^{-9}T^2 \quad [60°T < T < 80°F]$

The expected flow rate was calculated from eq. 9 and the measured column, downcomer and pool temperatures. The curve fit relation was used for viscosity and density. This flow rate was compared to that actually measured. Table I shows that the calculated velocity agrees very well with the measured velocity. Appendix 5 contains the computer program used to generate Table I.

The thermosiphoning mass flow rate, and ingoing and outgoing water temperatures were measured to calculate the heat leaving:

(eq. 6) $\dot{Q} = \dot{m}c_p(T_{out} - T_{in})$

Equations 2 and 6 were used to calculate the thermosipnoning rate in the computer model.

TABLE I

| READING | DGH | VCALC | VEXP | DIFF | RATIO |
|---|---|---|---|---|---|
| 1 | 0.091 | 0.0598 | 0.0535 | 11.8 | 0.895 |
| 2 | 0.067 | 0.0460 | 0.0472 | -2.6 | 1.026 |
| 3 | 0.076 | 0.0519 | 0.0471 | 10.2 | 0.908 |
| 4 | 0.098 | 0.0639 | 0.0654 | -2.2 | 1.023 |
| 5 | 0.109 | 0.0699 | 0.0702 | -0.4 | 1.004 |
| 6 | 0.110 | 0.0710 | 0.0673 | 5.5 | 0.948 |
| 7 | 0.109 | 0.0702 | 0.0678 | 3.5 | 0.966 |
| 8 | 0.105 | 0.0684 | 0.0601 | 13.7 | 0.879 |
| 9 | 0.091 | 0.0608 | 0.0570 | 6.7 | 0.937 |
| 10 | 0.075 | 0.0514 | 0.0522 | -1.6 | 1.016 |
| 11 | 0.077 | 0.0529 | 0.0487 | 8.6 | 0.921 |
| 12 | 0.085 | 0.0572 | 0.0585 | -2.2 | 1.022 |
| 13 | 0.095 | 0.0627 | 0.0625 | 0.4 | 0.996 |
| 14 | 0.100 | 0.0650 | 0.0637 | 2.1 | 0.980 |
| 15 | 0.102 | 0.0659 | 0.0645 | 2.2 | 0.978 |
| 16 | 0.100 | 0.0648 | 0.0631 | 2.7 | 0.974 |
| 17 | 0.097 | 0.0630 | 0.0625 | 0.8 | 0.992 |
| 18 | 0.100 | 0.0639 | 0.0617 | 3.5 | 0.966 |
| 19 | 0.097 | 0.0622 | 0.0617 | 0.8 | 0.993 |
| 20 | 0.090 | 0.0582 | 0.0588 | -0.9 | 1.010 |
| 21 | 0.086 | 0.0560 | 0.0560 | 0.1 | 0.999 |
| 22 | 0.078 | 0.0512 | 0.0536 | -4.5 | 1.047 |
| 23 | 0.072 | 0.0480 | 0.0539 | -11.0 | 1.124 |
| 24 | 0.065 | 0.0438 | 0.0447 | -2.0 | 1.021 |
| 25 | 0.065 | 0.0440 | 0.0449 | -1.9 | 1.019 |
| 26 | 0.063 | 0.0431 | 0.0484 | -11.0 | 1.123 |
| 27 | 0.070 | 0.0475 | 0.0455 | 4.5 | 0.957 |
| 28 | 0.071 | 0.0482 | 0.0482 | 0.1 | 0.999 |
| 29 | 0.070 | 0.0475 | 0.0479 | -0.7 | 1.007 |
| 30 | 0.074 | 0.0467 | 0.0521 | -10.4 | 1.116 |
| 31 | 0.071 | 0.0449 | 0.0534 | -15.9 | 1.189 |

## RADIATION INTO THE WATER COLUMN

Net radiation into the water column can be calculated from the set of equations:

$$\text{(eq. 7)} \quad \sum_{j=1}^{n} \left( \frac{\delta_{Kj}}{\varepsilon_j} - F_{K-j} \frac{1-\varepsilon_j}{\varepsilon_j} \right) \frac{Q_j}{A_j} = \sum_{j=1}^{n} (\delta_{Kj} - F_{K-j}) \sigma T_j^4$$

where $F_{i-j}$ = view factor from surface i to surface j

$A_i$ = area of surface i

$\varepsilon_i$ = emmissivity of surface i

$Q_i$ = net heat flux from surface i

n = number of surfaces

If the surface absorbtivity is equal to its emmissivity these equations give the exact radiative heat transfer.

Difficulties creep in when these equations are applied to a real enclosure. View factors are often difficult to determine. Emmissivities of wall paints at about 78°F (25°C) have not been exactly determined. Dark paint can range between .85 and .96. White paint ranges between .80 and .92. (6)

ASHRAE (7) suggests approximating wall temperatures at the air temperature so that radiative transfer into the water column can be expressed as:

$$\text{(eq. 8)} \quad \dot{Q} = \alpha A \sigma (\bar{T}_a - \bar{T}_c)$$

where $\alpha$ = column absorbtivity

A = column surface area

$\sigma$ = Stefan-Boltzmann constant

$\bar{T}$ = average air temperature

$\bar{T}_c$ = column temperature

This works well for some conditions. However, wall capacitance, wall thermal conductance, infiltration, insolation, the outside temperature history, and the presence of thermal storage mass can all effect the relationship between wall temperature and air temperature. Since radiative transfer is dependent on the forth power of temperature the use of an average temperature for its calculation will not always yield an accurate answer.

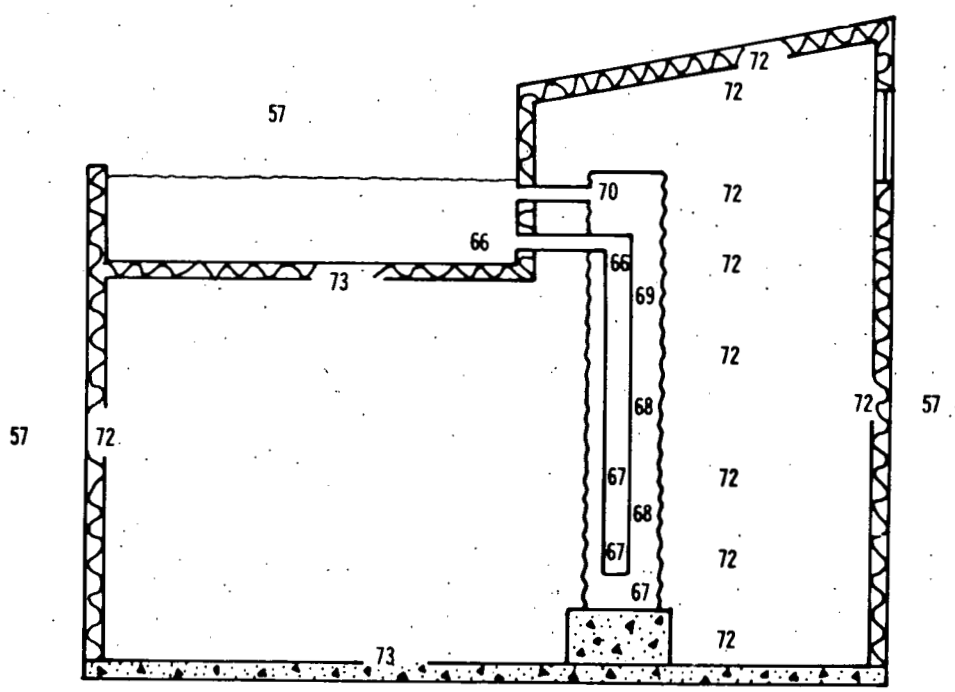


Figure 6. Early Morning Temperatures

Figure 6 shows the measured air and wall temperatures of the test building at 5 a.m. in the morning. In this case there is very little difference between wall temperature and the air temperature. Radiation calculated from the average air temperature will yield similar results to the enclosure analysis.

Figure 7 shows this same building at 3:00 p.m. in the afternoon. The wall temperatures are very different from the average air temperature. The radiative heat transfer to the column calculated from the average air temperature will be greater than the enclosure analysis indicates.

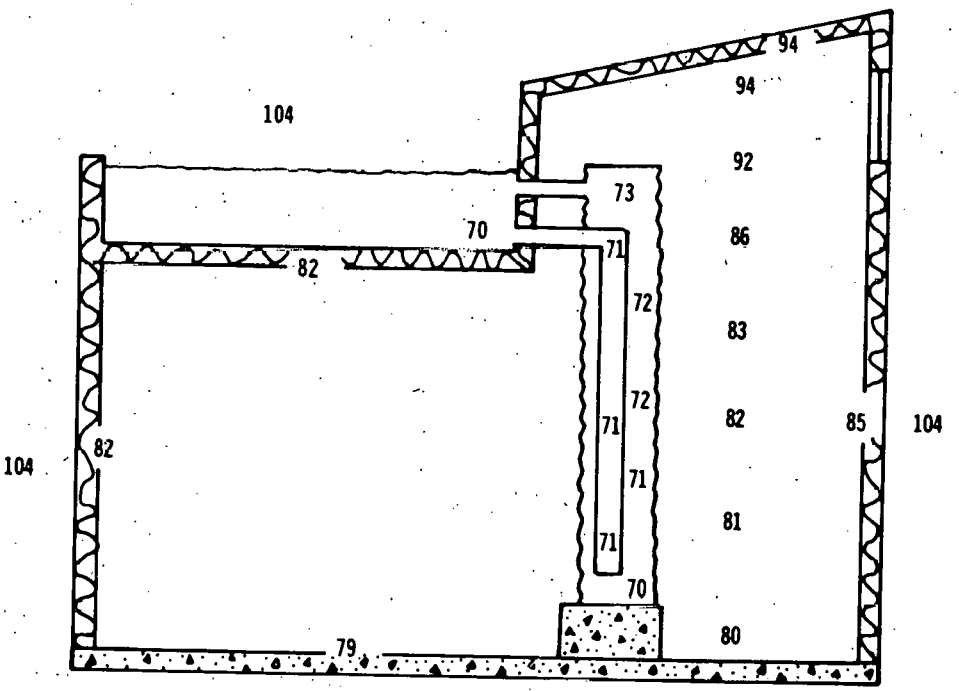


Figure 7. Afternoon Air Temperatures

The accuracy of using air temperature as an approximation for radiation was tested by comparing the transfer rate to that obtained by using an enclosure analysis.

Since the column temperature varied by less than 3°F (2°C) it was modeled at one average temperature. Each of the 4 walls were assumed to be at a constant temperature equal to that measured 4 ft. from the floor. The ceiling was divided into two isothermal areas, one exposed to the sky and one under the roof pond. The floor was modeled at one temperature. Since, presumably, the surfaces were not isothermal some error will be introduced by these assumptions.

Figure 8 shows hour-by-hour calculations of radiative heat transfer. The wall and column emmissivities were .91 and .93.

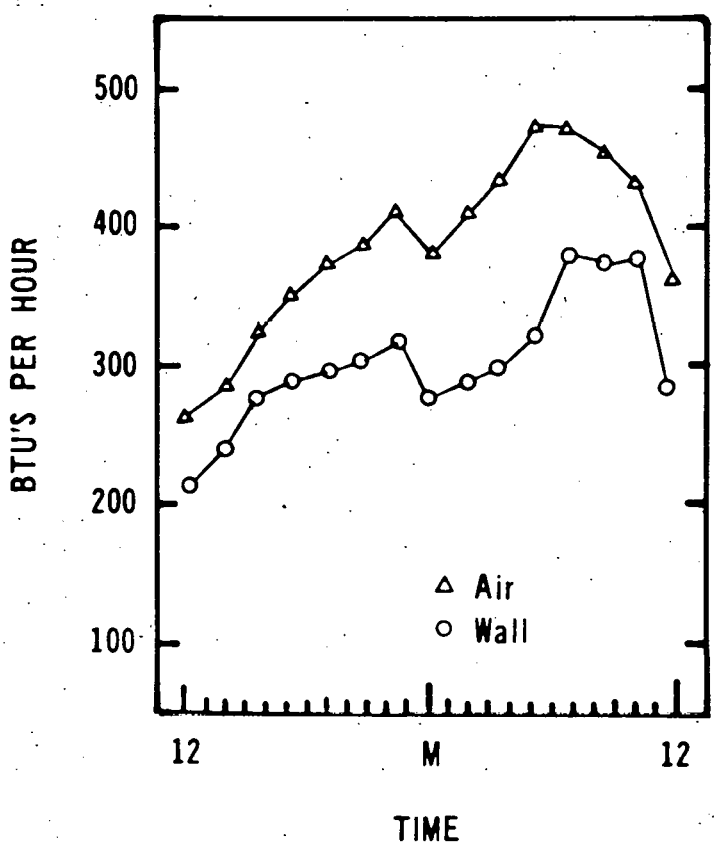


Figure 8. Radiation: Enclosure and Air Temperature Calculations

This graph shows that using the average air temperature for radiation calculation overestimates the heat transfer into the thermal mass for this particular building. This error is less during the night when wall temperatures are more uniform.

## CONVECTION INTO WATER COLUMN

Heat is transferred from the indoor air to the water column by convection, through the corrugated metal column wall by conduction and to the water by convection. The free convection heat transfer coefficient from air to a vertical cylinder can be found from (4):

(Eq. 9) $Nu = 0.13\ (GrPr)^{.33}$ $\qquad (10^8 \quad GrPr \quad 10^{12})$

Since the water column is 8 feet (2.4 m) tall, GrPr $10^9$ and the free convection is in the turbulent region. The corrugations may increase the heat transfer slightly. (5) This relation has been simplified for air at $70^{\circ}F$ ($21^{\circ}C$) (4):

(eq. 10) $h_a = 0.19\ (T_a - T_c)^{.33}$ $\qquad$ $Btu/ft^2\text{-}hr\text{-}^{\circ}F$ $(GrPr \quad 10^9)$

where:

$h_a$ Heat transfer coefficient ($Btu/ft^2\text{-}hr\text{-}^{\circ}F$)

$T_a$ air temperature

$T_c$ column temperature

Equation 9 is often used in place of equation 8. Notice there is no dependence on the surface geometry in equation 9. Since conditions are evaluated at $70^{\circ}F$, equation 9 yields a slightly lower heat transfer coefficient than equation 8.

Since the water column is within an enclosure, convective air loops may be set up between the cool column and the warmer walls. This will increase the velocity of the air moving past the column and thus increase the convective heat transfer rate. Thus, equation 9 probably underestimates convective heat transfer. This hypothesis will be discussed further.

The thermal resistance per unit area between the air and the column surface is the inverse of the heat transfer coefficient:

(eq. 11) $R_a = 1/h_a$

where $R_a$ is the thermal resistance between the interior air and the column surface. Since the temperature difference is usually less than $10^{\circ}F$ ($6^{\circ}C$) this resistance is about:

(eq. 12) $R_a \sim 2.4$ $(ft^2 \cdot hr \cdot {}^{\circ}F)/BTU$

Conduction through the .064" (.16 cm) thick metal column skin is 4 orders of magnitude faster than convection from the air to the surface of the column. The conductivity of steel is 26.2 $BTU/{}^{\circ}F$ ft hr so that the resistance:

(eq. 13) $R_c \quad L/K = 2.0 \times 10^{-4}$ $(ft^2 \cdot hr \cdot {}^{\circ}F)/BTU$

where $R_c$ is the thermal resistance of the column wall.

The heat transfer coefficient from the column skin to the water can be found from the free convection relationship of equation 9. At a $10^{\circ}$ difference between column and water temperature and a water temperature of $73^{\circ}F$ ($23^{\circ}C$) the resistance, $R_2$ is $1.9 \times 10^{-4}$ $(ft^2 \cdot hr \cdot {}^{\circ}F)/BTU$. Again, this resistance is four orders of magnitude less than the air to column surface resistance.

Because the air to column resistance dominates convective heat transfer into the water column, conduction and convection to the water can be neglected.

The water column was placed on 1/2" thick plywood on hollow cinder blocks. Thus, conduction into the base of the column is

negligible. Heat transfer into the cylinder top was neglected since the 1 inch air gap between the plastic cap and the water surface was assumed to act as an insulating space.

If a heat balance is done on the water column it is found that the heat entering the column from radiation and convection must equal the change in the column heat content plus the heat leaving by thermosiphoning.

The change in heat content was determined from the hourly change in temperatures of the column

$$\text{(eq. 14)} \quad \Delta Q = m_c c_p (\overline{T}_2 - \overline{T}_1)$$

where: $m_c$ = mass of water in column

$c_p$ = specific heat of water

$\overline{T}_2$ = new average water temperature

$\overline{T}_1$ = old average water temperature.

From this, the hourly heat transfer rate into the water column can be calculated.

Figure 10 shows calculated heat transfer rates (based on measured air, wall and column temperatures) and the experimentally determined heat transfer rates. The lowest curve results from adding the convective transfer ($h = .19\ (\Delta T)^{1/3}$) to the enclosure analysis radiation. The other curve results from adding this convective transfer to radiation calculated from the average air temperature. The solid line represents the experimental heat transfer rate.

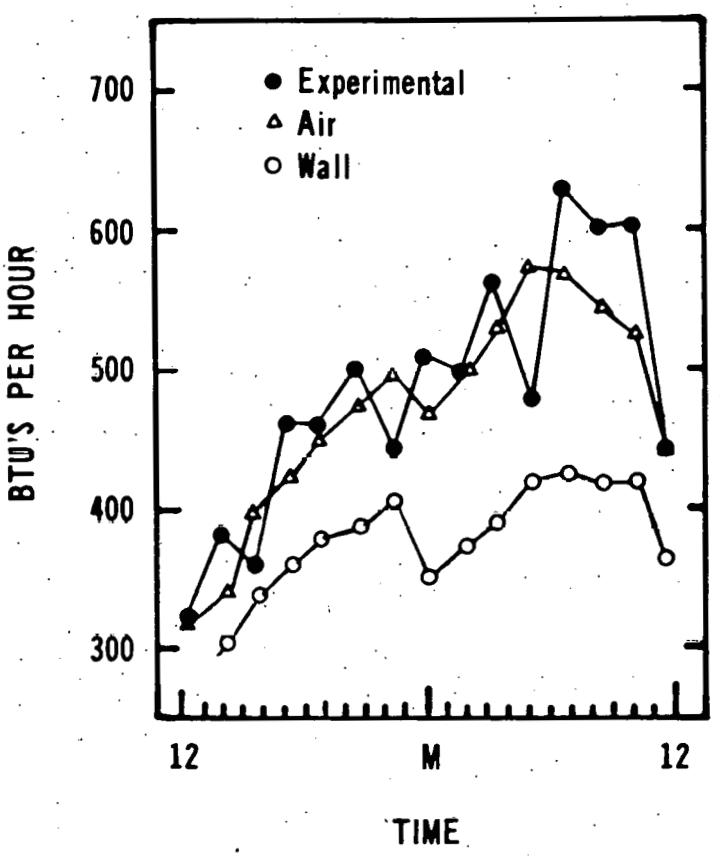


Figure 10. Total Heat Into Column

The accurate enclosure analysis radiation added to the conventional convective heat transfer underestimates the total heat transfer. When the (incorrect) air temperature radiation is added to the conventional convective transfer, the calculated result agrees very well with the experiment. This is because radiation is overestimated to compensate for the underestimation of convection. Thus, this method gives a correct answer for the wrong reasons.

This discrepancy is greatest when the wall temperature is much higher than the mass temperature. This lends support to the hypothesis that convection loops within the enclosure are increasing the heat transfer rate.,

This analysis implies that the heat transfer coefficient is consistantly higher than that predicted by equation 4. However, this is only an indication that more work should be done on this question since there are many uncertainties involved in this analysis. A detailed error analysis appears in Appendix 3. The water column contains so much mass that a $0.1^{o}F$ change in temperature can mean a change of 86 BTU's. Since temperatures were read to the nearest $0.1^{o}F$ and the total hourly change in column energy content averaged 130 BTU/hr this introduces a possible 66% error. The thermosiphoning rate was much higher (300 - 600 BTU/hr) so that the impact of this error on the calculated convection rate is about 20%. The fact that the trend is consistant argues that the actual error was less than this.

Calculated enclosure radiation could add additional error to the convection. Emmissivities were unverified and the view factors were approximate. Modeling the columns and enclosure as 10 isothermal surfaces introduces an unknown error. In any case, it is clear that using air temperature instead of surface temperatures for radiation calculations will overestimate radiative transfer in this situation. The computer model uses average air temperature for the calculation of radiation and convection into the water column.

## EVAPORATION

The Reynolds analogy for heat transfer can be extended to convective mass transfer:

(eq. 14) $$\frac{Sh}{Re \cdot Sc} = \frac{Nu}{Re \cdot Pr} = \frac{f}{2}$$

where: Sh = Sherwood number

Sc = Scranton number

Re = Reynolds number

Pr = Prandtl number

Nu = Nusselt number

f = friction factor

This is adequate for Pr 1, and small temperature gradients. Chilton and Colburn modified the above relationship:

(eq. 15) $$\frac{Sh}{Re}(Sc)^{-1/3} = \frac{Nu}{Re}(Pr)^{-1/3} = f/2$$

For water vapor in air this reduces to:

(eq. 16) $$\frac{h}{g} = 0.21$$

where h = convective heat transfer coefficient

g = mass transfer coefficient

Although the heat transfer correlation to friction isd not accurate for Reynolds numbers less than 10,000 it is felt that equation 14 will give a good estimate at lower Reynolds numbers if the heat transfer coefficient can be determined from some other relationship. (2) Equation 16 is used in the computer simulation. The energy transfer rate from evaporation is

(eq. 17) $$Q = g\, i_{fg}(w_o - w_p)$$

where: g = mass transfer coefficient

$i_{fg}$ = heat of vaporization of water

$w_o$ = outside absolute humidity

$w_p$ = absolute humidity of saturated air at pool temperature

A curve fit for $i_{fg}$ was used.

(eq. 18) $i_{fg} = 1091.40 - .495T - 5.00 \times 10^{-4} T^2$ BTU/$lb_m$

$[60°F < T < 80°F]$

The absolute humidity (w) was found from the relationships:

(eq. 19) $P_{vs} = \exp[-3.078 + 4.527 \times 10^{-2} T - 8.0101 \times 10^{-5} T^2]$

where $P_{vs}$ is the saturated vapor pressure in inches of $H_g$ at T(°F) and $35°F \leq T \leq 74.97°F$

(eq. 20) $P_{vs} = \exp [-3.0006 + 4.310 \times 10^{-2} T - 6.5016 \times 10^{-5} T^2]$

$74.97 < T \leq 110°F$

(eq. 21) $w_s = .622\ P_{vs}/(P - P_{vs})$ $lb_m$/cu. ft dry air

where P = total pressure

(eq. 22) $w = .622 \left[ \left( \frac{100}{RH} \right) \left\{ 1 + \frac{.622}{w_s} - 1 \right] ^{-1} lb_m/cu. ft$

where RH = Relative Humidity.

Equation 21 was used to find the saturated absolute humidity over the pool. Equation 22 could be used to calculate the outside absolute humidity from the relative humidity. In this program the outside absolute humidity calculated from wet and dry bulb temperatures and used as an input.

## CONVECTION INTO ROOF POND

The roof pond can be modeled as an isothermal flat plate. It is difficult to decide whether the convection is free or forced since wind speed varies and the shades may slow the air movement over the pool. It is clear that the heat transfer will be equal to or greater than that which the free convection relationship yields.

During the day when the pool is warmer than the outside air the following relationship would apply for turbulent free convection heat transfer. (7)

(eq. 24) $h = 0.19\ (\Delta T)^{0.33}$

where: $h$ = the heat transfer coefficient BTU/°F-ft$^2$-hr

$\Delta T$ = the difference between air temperature and pool temperature

During the night when air temperatures drop below the pool temperatures the following turbulant free convection relation would apply: (7)

(eq. 25) $h = 0.22\ (\Delta T)^{0.33}$

The average summer wind speed in the Sacramento area is 12.5 ft/sec (3.8 m/s). (8) Measurements taken by previous researchers indicate that the shade used on the test building roof pond reduces the wind velocity over the water to an average of about 2 ft/sec. (9)

The forced convection correlation for air over a horizontal isothermal surface is: (11)

(eq. 26) $h_a = 0.664\ Re_L^{1/2} Pr^{1/3} \frac{k_a}{L_p}$

(Laminar Re < $10^6$)

or:

(eq. 27) $h_a = 0.036\ Re_L^{4/5} Pr^{1/3} \frac{k}{L}$

(Turbulent Re > $10^6$)

where k = thermal conductivity of air

L = plate length

If the laminar equation is evaluated for a 68°F (20°C) and 80°F (27°C) air this yields

(eq. 28) $h = .69 \sqrt{v/L} = .28 \sqrt{v} \frac{BTU}{°F\ hr\ ft}$ [v < 28 ft/sec]

where v is the velocity in feet per second. For a velocity of 2 ft/sec h = .4 BTU/°F hr $ft^2$. If the outside temperature is more than 9°F (5°C) different from the pool temperature the free convection will be greater than the forced convection. In this case the computer program chooses the greater of the two heat transfer coefficients.

## CONDUCTION

Into Pool:

The pool edges are insulated with R19 fiberglass batts and will gain (or lose) heat from the outside air.

(eq. 29) $\dot{Q} = (1/R)\ A\ (T_a - T_b)$

where R = 20 $(°F \cdot hr \cdot ft^2)/BTU$

A = 32 $ft^2$ area

$T_a$ = outside temperature

$T_b$ = pool temperature

The pool bottom is insulated from the living space by R-19 fiberglass batts and will transfer heat according to the above relation. In this case: the area is 60 $ft^2$ (2.2$m^2$) and T represents the inside temperature.

The top edges of the sheet metal pool container extend into the air and may act as fins by conducting heat into the pool. This effect was neglected.

Into Downcomer:

Since the ABS downcomer is immersed within the column heat will conduct across the plastic to heat it according to the equation:

(eq. 30) $\dot{Q} = \frac{1}{R} A\ (T_c - T_d)$

where R = conductive and convective resistance of the ABS plastic and water
$T_c$ = column water temperature
$T_d$ = downcomer water temperature
A = surface area of downcomer

This relation was used in the computer simulation. It was assumed that convection loops set up within the column between the warm column and the cooler downcomer would result in the conducted "coolth" from

the downcomer falling down to the lowest column node. Thus, the conduction was calculated node by node but the total heat was removed only from the bottom column node.

## NET RADIATION INTO POOL

Although the shades block direct sun from the pool, diffuse radiation enters it during the day. The shades heat up and radiate into the pool. At night the pool can lose heat by radiation to the cooled shades and the small amount of visible sky. The net radiation into the pool was measured and this constituted one of the computer inputs.

## BUILDING HEAT LOAD

The test building heat load was calculated according to ASHRAE standards to yield an effective U x A value of 74 BTU/$^{o}$F-hr. The heat entering the test building air was calculated by

(eq. 31) $Q = U \times A \ (T_{out} - T_{in})$

This treatment does not take into account the lag induced by wall capacitance nor the effect of insulation on the walls and roof. It was not the intent of this work to model the building itself.

## COMPUTER SIMULATION

The computer simulation is listed in Appendix 2. The Cool Pool system was divided into ten nodes (see Figure 11). The column was divided into 5 slices; the downcomer into 3 slices; the interior air was modeled as one node and the roof pond makes the tenth node. Each node was assumed to be at a uniform temperature. A heat balance was done for each node to generate a system of ten nonlinear first order differential equations. These equations were solved by a library program. A list of the nodes and their heat and mass transfer processes follows:

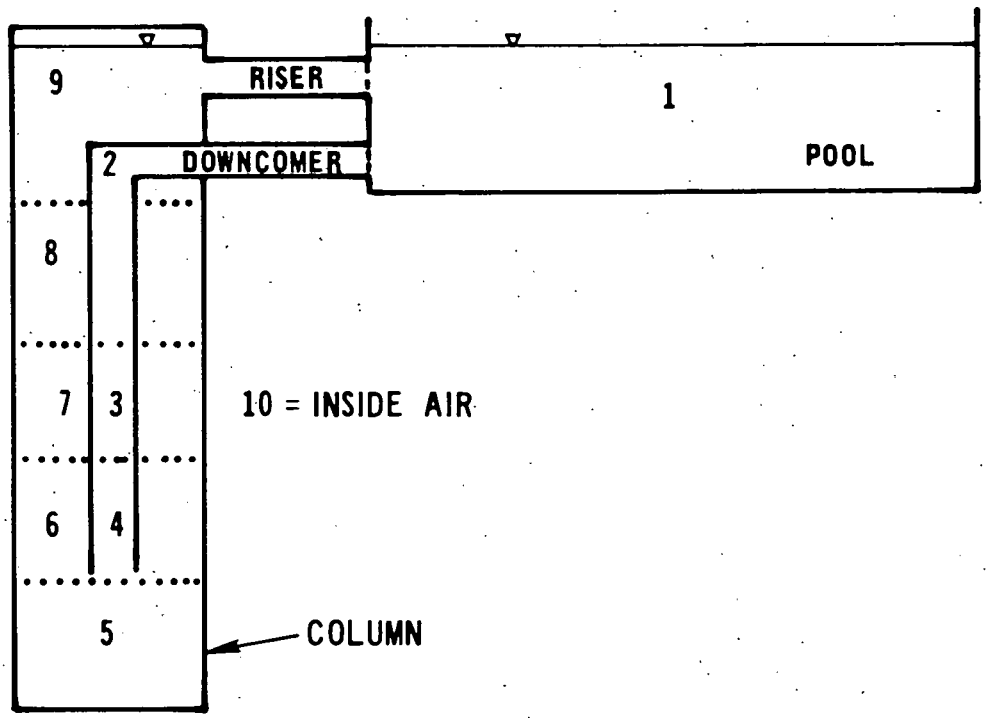


Figure 11. Computer Nodes

Node 1 The Roof Pond

A) mass flow from volumn top (eq. 2,6)

B) mass flow to downcomer top (eq. 2,6)

C) evaporation to outside air (eq. 17)

D) convection to outside air (eq. 24-26)

E) net radiation into pool (experimental)

F) conduction to living space (eq. 29)

G) conduction to outside (eq. 29)

Node 2-4 The Downcomer

A) mass flow in (eq. 2,6)

B) mass flow out (eq. 2,6)

C) conduction from water column (eq. 30)

Node 5-9 The Column

A) mass flow in (eq. 2,6)

B) mass flow out (eq. 2,6)

C) radiation to building interior (eq. 8)

D) convection to interior air (eq. 10)

E) conduction to downcomer from lowest node only (eq. 30)

Node 10 The Interior Air

A) radiation from column (eq. 8)

B) convection from column (eq. 10)

C) building load (eq. 31)

Hourly Inputs

C(2) outside temperatures

C(3) absolute humidity

C(4) net radiation into pool

C(5) building heat load

The specifiable parameters such as cool pool geometry are listed in Appendix 2. These parameters can be read in so that Cool Pool systems of varying sizes can be simulated. Appendix 2 also lists the variable values such as viscosity and density which are calculated each hour or each time step depending on their importance and impact.

The model was verified by initializing the ten node temperatures to match the experimentally measured temperatures. The program was allowed to simulate 24 hrs. of performance using hourly inputs (outside temperature, humidity, net radiation into pool, and building load) which were the same as those measured during the experiment. The node temperatures and the thermosiphoning rate were then compared to the experimental values with very good agreement.

Heat transfer from the air to the column is calculated using average air and column temperatures. This gives good results and eliminates the necessity of modeling stratification in the air. From figures 6 and 7 it can be seen that air stratification is dependent on the outside temperature history, building design and capacitance (to name a few factors). Figure 12 shows the average of the experimental air temperatures compared to the computer simulation.

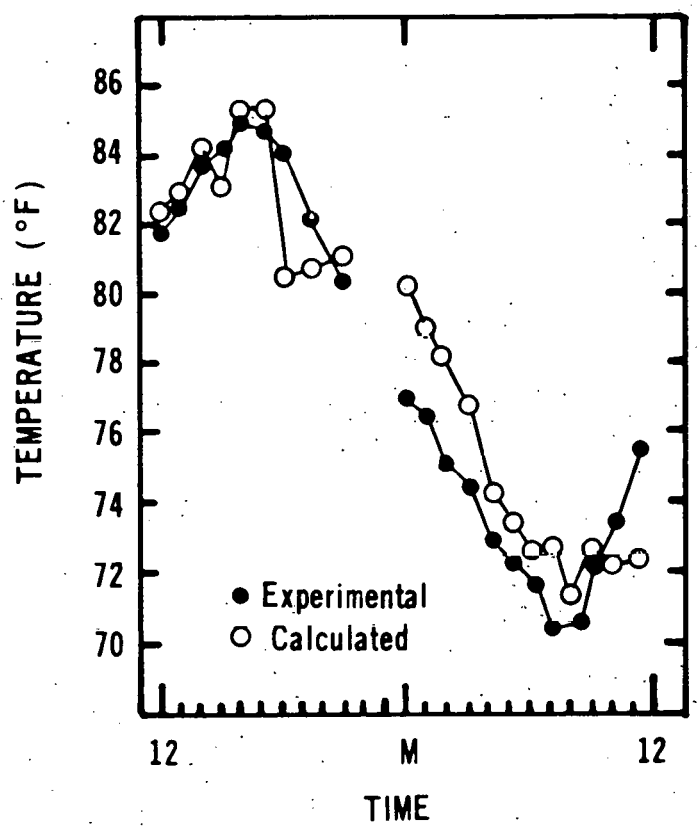


Figure 12. Average Air Temperatures

Due to instrument difficulties no data was recorded at 10 p.m. and 11 p.m. The air temperature was extremely sensitive to the building load estimate since it had little capacitance and factors such as infiltration could only be crudely estimated. However the greatest deviation in temperature was 2.7°F (1.5°C)

Conduction from the column to the downcomer was calculated for adjacent nodes but the net heat transfered into the three downcomer nodes was only subtracted from the lowest column node. This simulates convective loops within the column which enhance water stratification. Mass leaves the node at the node temperature and enters the node of the previous node's temperature. Then the new isothermal node temperature is determined. This method yields close agreement to the measured column temperatures as shown in figure 13.

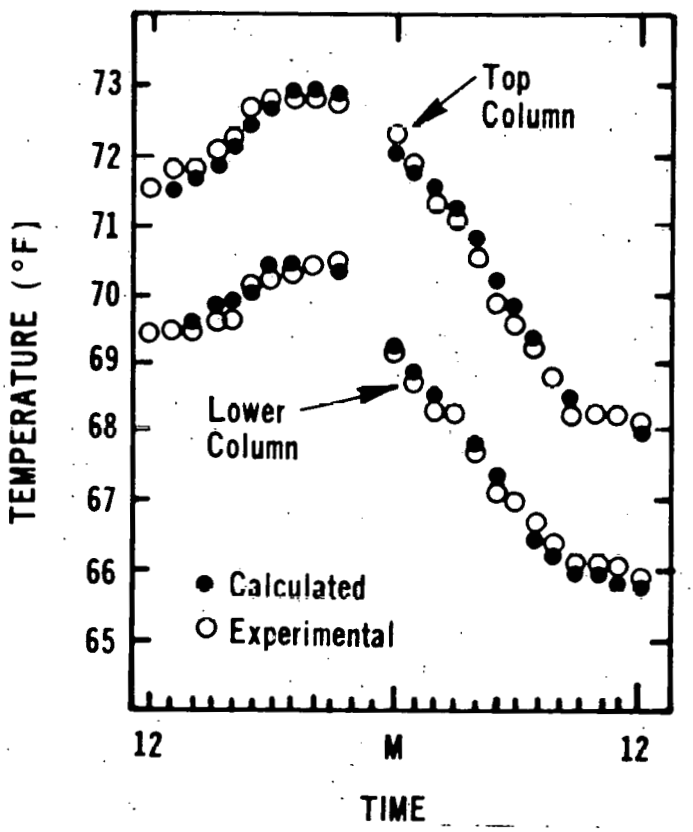


Figure 13. Column Temperatures

Figure 14 shows experimental and pool temperatures. Again, there is excellent agreement. In this case the pool was probably larger than required for the heat load from thermosiphoning. Thus, the rest of the system had little impact on it. The reverse is not true.

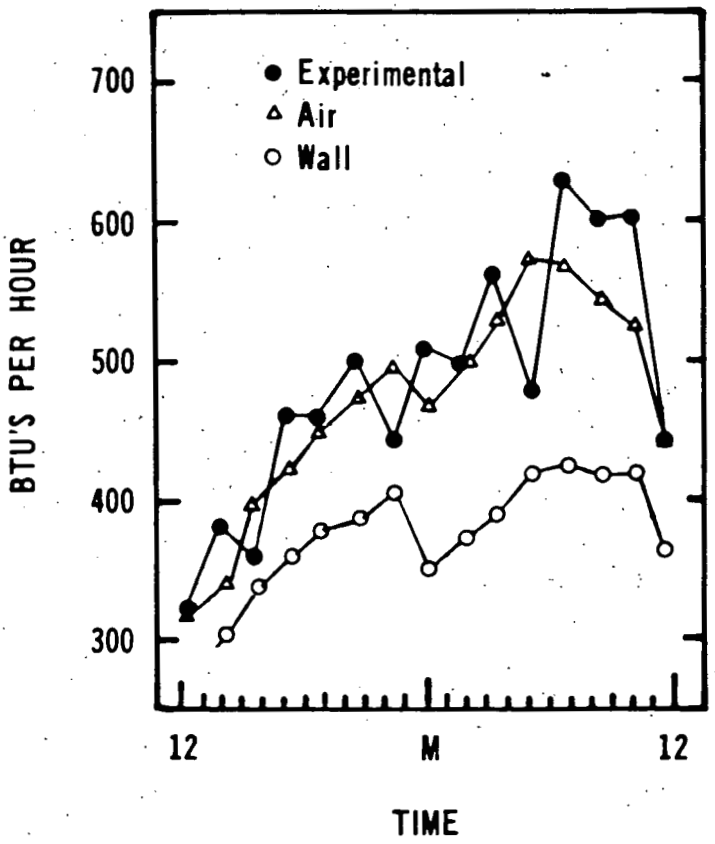


Figure 14. Pool Temperature

The pool temperature was critical in determining the thermosiphoning rate since the colder downcomer water was greater than the pressure difference was. Figure 14 shows the calculated vs. experimental thermosiphoning rate. Near midnight, the calculated rate was 15% lower than the measured rate. The rest of the time there was much better agreement.

Figure 15 shows the downcomer temperatures which agreed closely.

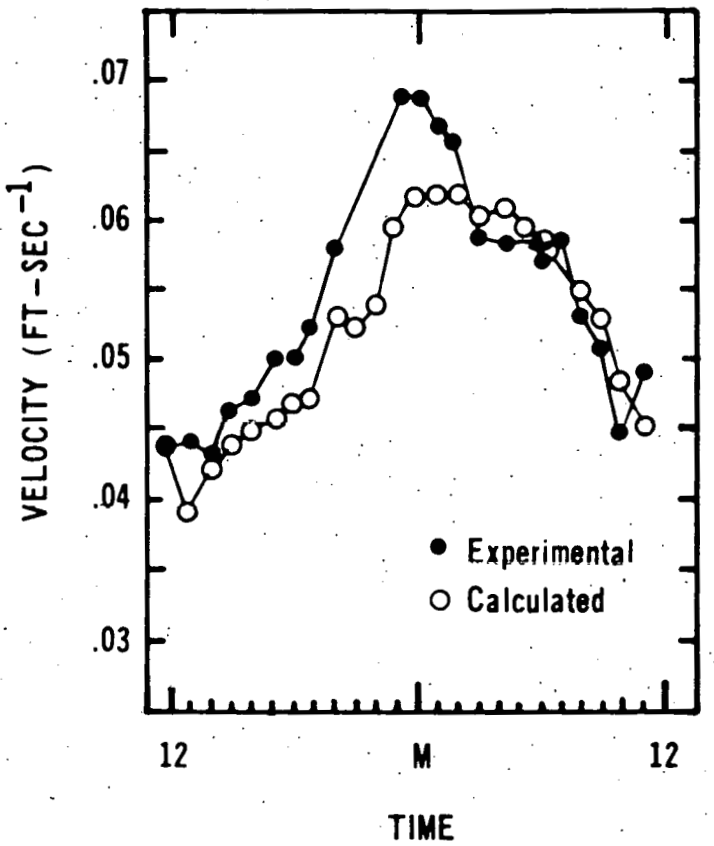


Figure 15. Thermosiphoning

Figure 16 shows the most important calculation, heat absorbed by the column. This is the factor which determines sizing. As discussed earlier, the experimental calculation could be off by 20% or more. The agreement with simulated values is well within 20%.

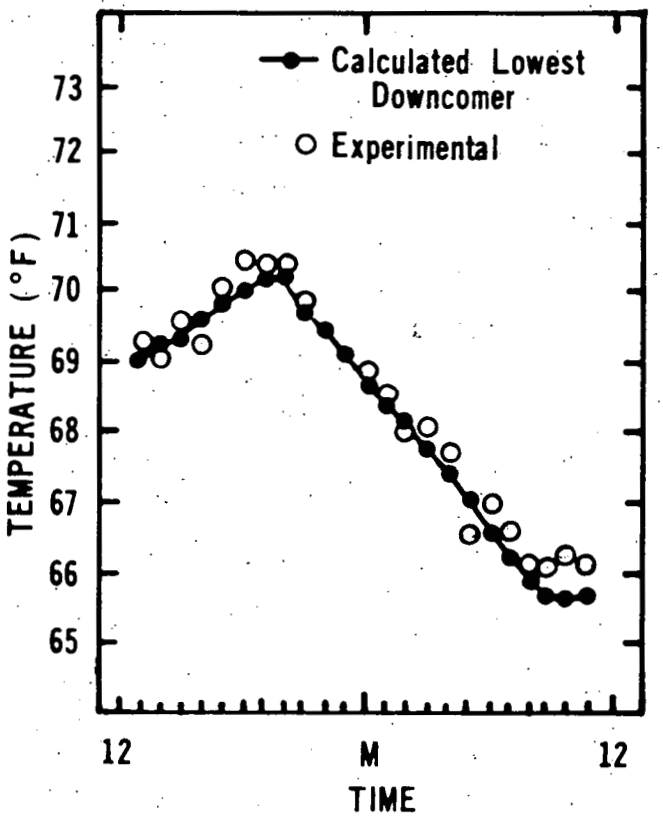


Figure 16. Downcomer Temperatures

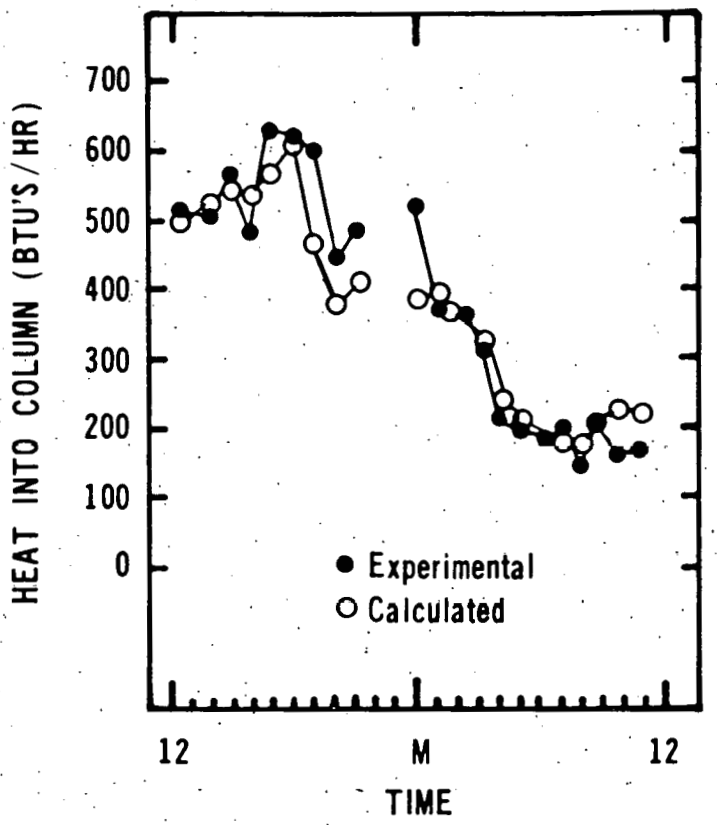


Figure 17. Total Heat Into Column Wall

# CONCLUSION

This work has increased the experimental data available on the thermosiphoning roof pond. Although conventional methods for calculating the thermosiphoning rate, heat transfer and evaporation do a good job modeling this system, it is clear that convective heat transfer relationships for enclosed spaces need to be developed.

Now that a good computer simulation is available for this system it will be easy to input other climate values and system parameters in order to size the Cool Pool for different regions.

# A P P E N D I X  I

## TEST BUILDING

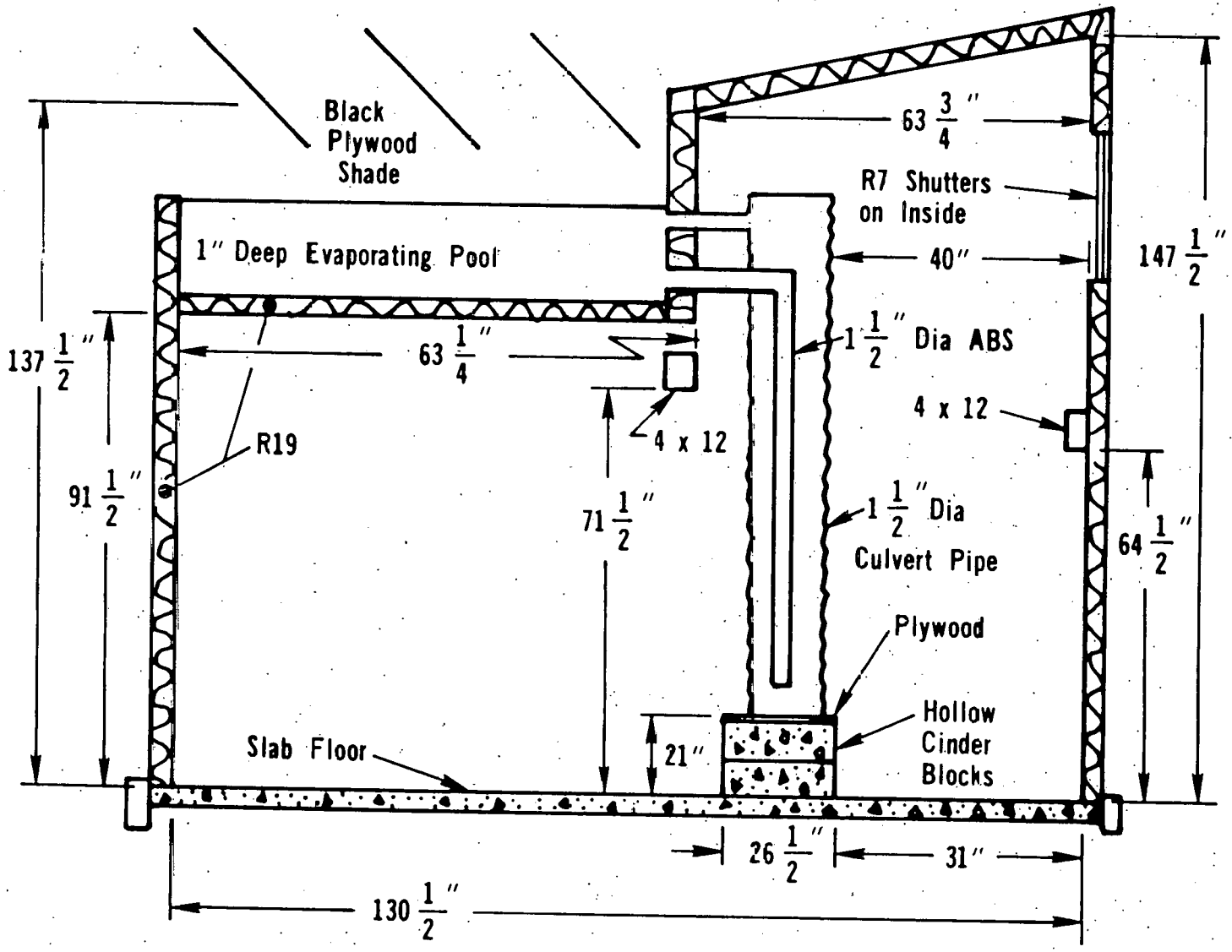
Black
Plywood
Shade
1" Deep Evaporating Pool
63 3/4"
R7 Shutters
on Inside
40"
147 1/2"
1 1/2" Dia ABS
4 x 12
137 1/2"
63 1/4"
R19
4 x 12
91 1/2"
71 1/2"
1 1/2" Dia
Culvert Pipe
64 1/2"
Plywood
Hollow
Cinder
Blocks
21"
Slab Floor
26 1/2"
31"
130 1/2"

SECTION OF TEST BUILDING

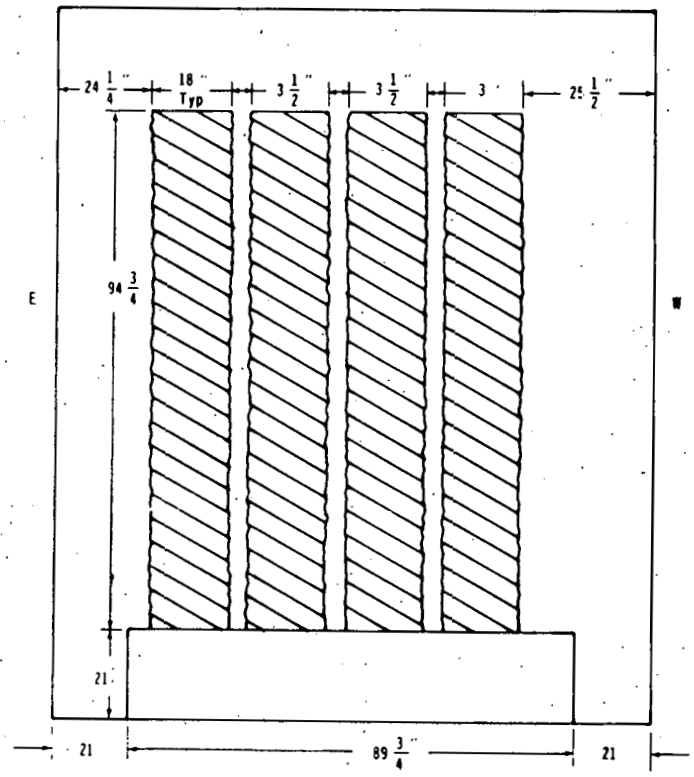


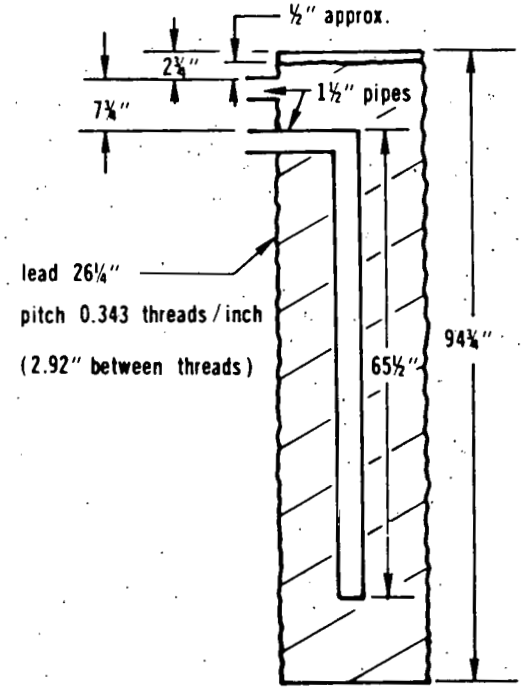


OD peaks $18\frac{7}{8}$"

OD valleys $17\frac{1}{8}$"

TUBE